Table 2 Profile of patients with SIADH

No.	*Age (years)*	*Gender*	*SCT*	*HLA mismatch*	*Disease*	*Conditioning regimen*	*GVHD prophylaxis*	*At the time of SIADH*				*Neurological sequelae*
								Na (mmol/l)	*Day*	*WBC ($\times 10^9$/l)*	*Symptom*	
1	4	M	U-BMT	0	JMML (CP)	TBI+VP16+CY	CsA+short MTX	122	40	2.8	Nausea	Dead
2	10	M	R-BMT	1	AML (CR1)	TBI+VP16+CY+ATG	CsA+short MTX	121	60	2.5	Nausea	None
3	1	M	U-CBSCT	0	WAS	BU+CY	CsA+short MTX	110	32	1.6	Seizure	None
4	7	F	U-CBSCT	1	AML (CR2)	BU+L-PAM	CsA+mPSL	118	41	4.2	None	Dead
5	1	M	U-CBSCT	1	NHL (CR3)	TBI+VP16+CY	CsA+mPSL	120	15	1.0	Nausea	DD, seizure
6	5	F	U-CBSCT	1	AML (CR2)	BU+L-PAM	CsA+mPSL	121	18	1.0	Nausea	None
7	1	M	R-BMT	1	Aplastic anemia	TLI+ATG+CY	CsA+short MTX	106	74	3.3	Nausea	None
8	3	F	U-BMT	0	Aplastic anemia	TBI+ATG+CY	FK506+short MTX	115	27	4.2	Nausea	None
9	7	F	R-PBSCT	1	ALL (CR1)	ATG+CY	FK506+short MTX	115	54	0.2	Nausea	None
10	3	M	R-BMT	0	ALL (CR1)	TBI+VP16+CY	CsA+short MTX	121	52	2.9	Nausea	None
11	9	F	U-CBSCT	2	NB (CR1)	CBDCA+VP16+L-PAM	CsA+mPSL	117	19	0.1	Nausea	None
12	0	M	U-CBSCT	0	WAS	BU+CY+ATG	CsA+mPSL	122	19	0.9	Nausea	None
13	10	F	U-BMT	0	ALL (CR1)	TBI+VP16+CY	FK506+short MTX	123	31	6.4	Nausea	None
14	12	M	R-BMT	1	AML (CR2)	BU+L-PAM	FK506+short MTX	122	18	13.3	Nausea	Dead
15	2	M	R-BMT	1	Hurler Scheie	BU+CY+ATG	FK506+short MTX	123	35	2.7	Nausea	None
16	3	M	U-CBSCT	1	JMML (CP)	TBI+Ara-C+CY	CsA+mPSL	123	34	0.6	Seizure	Dead
17	6	M	U-CBSCT	1	ALL (CR2)	TBI+VP16+CY	CsA+mPSL	115	28	0.5	Somnolence	DD, seizure
18	14	F	U-CBSCT	2	CAEBV	Flu+VP16+TBI	CsA+mPSL	118	22	1.6	Seizure	Seizure
19	11	F	U-CBSCT	1	ALL (CR1)	TBI+VP16+CY	CsA+mPSL	117	15	1.2	Somnolence	None
20	7	M	U-CBSCT	1	ALL (non-CR)	TBI+VP16+CY	CsA+mPSL	120	17	2.4	Nausea	None
21	4	M	U-CBSCT	1	Aplastic anemia	Flu+L-PAM+TBI	CsA+mPSL	120	20	0.4	Seizure	DD, seizure
22	5	M	U-CBSCT	1	AML (CR3)	BU+L-PAM	CsA+mPSL	120	15	2.5	Rigidity of limbs	None
23	3	M	U-CBSCT	1	NB (CR1)	TBI+VP16+CY	CsA+mPSL	115	17	0.2	Seizure	None
24	15	M	U-BMT	1	ALL (CR3)	BU+L-PAM	FK506+short MTX	122	72	5.6	Nausea	Seizure
25	11	M	U-CBSCT	2	ALL (CR3)	TBI+VP16+CY	CsA+mPSL	123	21	2.3	None	None

Abbreviations: Ara-C = cytarabine; ATG = antithymocyte globulin; CAEBV = chronic active EBV infection; CBDCA = carboplatine; CBSCT = cord blood SCT; DD = developmental delay; FK506 = tacrolimus; Flu = fludarabine; JMML = juvenile myelomonocytic leukemia; L-PAM = melphalan; mPSL = methyl prednisolone; Na = sodium; NB = neuroblastoma; NHL = non-Hodgkin's lymphoma; TLI = total lymphoid irradiation; SIADH = syndrome of inappropriate antidiuretic hormone; VP16 = etoposide; WAS = Wiskott–Aldrich syndrome.

Table 3 Comparison between patients with CBSCT and BMT/PBSCT

	CBSCT (n = *15*)	*BMT/PBSCT* (n = *10*)
Gender		
Male	10	7
Female	5	3
Age (median, years old)	5	6
Minimum sodium level (median, mmol/l)	120	121.5
Onset of SIADH (median, day)	19*	46*
WBC at onset of SIADH (median, $\times 10^9$/l)	1.0*	3.1*
Severe symptom at SIADH	8*	0*
Neurological sequelae	4	1

Abbreviations: CBSCT = cord blood SCT; SIADH = syndrome of inappropriate antidiuretic hormone.
*$P<0.05$.

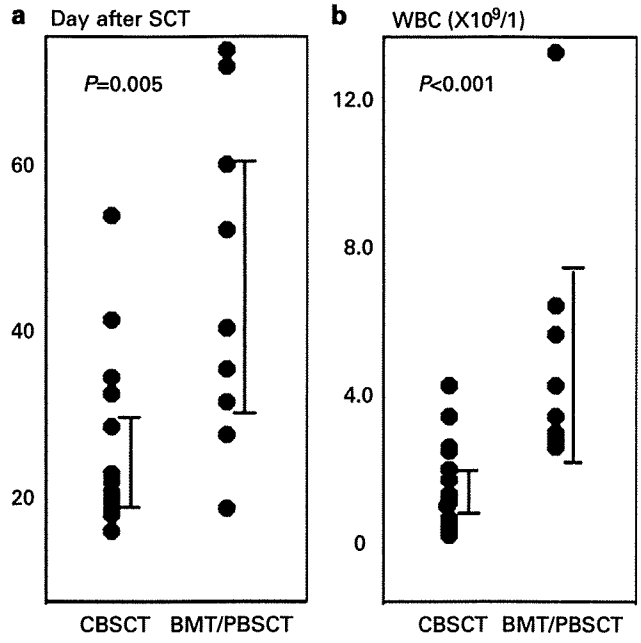

Figure 1 (a) Day of the onset of syndrome of inappropriate secretion of antidiuretic hormone (SIADH) following cord blood SCT (CBSCT) and BMT/PBSCT. (b) WBC at the onset of SIADH in patients with CBSCT and BMT/PBSCT.

Neurological sequelae occurred in 4 (26.6%) of the 15 patients receiving CBSCT, but in only 1 (10.0%) of the 10 patients after BMT/PBSCT. In analysis limited to survivors, neurological sequelae occurred in 4 (30.8%) of the 13 survivors after CBSCT, whereas it occurred in one (12.5%) of the eight survivors following BMT/PBSCT. These differences were not significant ($P>0.30$).

Discussion

In this study, we revealed for the first time the differences in SIADH clinical features between CBSCT and BMT/PBSCT treatments; patients receiving CBSCT had an earlier onset, a lower WBC count at the onset, and more severe symptoms than did those receiving BMT/PBSCT, and neurological sequelae were more frequent following SCT in survivors with SIADH than in those without SIADH.

Antineoplastic agents,[5,6] glucocorticoid,[7] hematological diseases[8–11] and other factors have been reported to be associated with SIADH. In this study, multivariate analysis revealed that only an alternative donor was independently associated with an increased risk of SIADH, whereas recipient age, gender, primary diseases, acute GVHD or drugs used in the peritransplant period were not independent risk factors (data not shown). These results, except for age, concurred with our previous report.[3] Although we have no available data at present, IL-6 has been reported to be involved in SIADH.[12–14] In addition, levels of cytokines such as IL-6 and tumor necrosis factor-α are known to be high in SCT from an HLA-mismatched donor or an unrelated donor.[15] These cytokines may induce SIADH following SCT, even though acute GVHD was not associated with the occurrence of SIADH.

In patients with SIADH following SCT, we found different SIADH clinical features following CBSCT and BMT/PBSCT. CsA and methylprednisolone were used more frequently in patients with SIADH following CBSCT, whereas antithymocyte globulin, FK506 and MTX were used more frequently in patients with SIADH following BMT/PBSCT ($P<0.04$). These drugs, however, were not associated with the occurrence of SIADH. Therefore, these clinical differences are likely due to the difference in the source of stem cells. A major difference in the outcome between CBSCT and BMT/PBSCT is recognized to be that CBSCT needs a longer period for hematological/immunological reconstitution than does BMT/PBSCT. However, the hypothesis that SIADH following SCT treatment is related to the expansion of donor cells is not likely because patients with SIADH following CBSCT had an approximate 3 week earlier onset and one-third of the WBC count at the onset compared to those with SIADH following BMT/PBSCT. The difference in cytokine reactions between CBSCT and BMT/PBSCT, such as pre-engraftment immune reactions proposed as an early phenotype of post-CBSCT immune reaction,[16,17] may explain these clinical differences.

We have previously shown significantly higher overall and event-free survival rates in patients with SIADH following SCT than those without SIADH.[3] In this study, although this conclusion was confirmed (data not shown), neurological sequelae following SCT occurred in survivors with SIADH more frequently than in those without SIADH. All patients with SIADH were promptly and appropriately treated with fluid restriction, diuretics or hypertonic saline (3% NaCl) and recovered from hyponatremia. NaCl (3%) was given to 23 of the 25 patients and its duration (median, 23 days; range, 1–116 days) was not associated with the source of stem cells or neurological sequelae (data not shown). Patients had no other metabolic disturbances, such as hypocalcaemia, hypomagnesaemia and hyper- or hypoglycemia. Only one patient diagnosed with human herpes virus 6 (HHV-6) encephalitis had a

neurological disorder other than SIADH. We therefore speculate that the causes of neurological sequelae are identical to those of SIADH. Although the precise basis for SIADH following SCT still remains unknown, there may be a pattern of cytokines inducing not only SIADH but also a GVL/tumor effect without GVHD. To test this hypothesis, it is important to determine whether there are significant differences in survival rates between malignant and non-malignant diseases. For this purpose, further analysis of a much larger number of patients with SIADH following SCT will be needed.

After the onset of SIADH, one patient (case 21) was diagnosed with HHV-6 encephalitis by PCR for HHV-6 using his cerebrospinal fluid. Although he was appropriately treated for SIADH and recovered from hyponatremia, he finally subsequently developed seizures and developmental delay. There are also a few reports of SIADH related to HHV-6 encephalitis.[18,19] Therefore, we speculate that, in this case, HHV-6 encephalitis caused SIADH and neurological sequelae. SCT often causes many neurological disorders,[20–22] some of which, such as CNS infections (bacterial and viral),[18,19,23–26] intracranial bleeding and drug toxicity (FK506),[27] have been reported to be associated with SIADH. Thus, subclinical neurological disorders might be present in these patients and elude diagnosis, although we were unable to demonstrate any neurological disorders in other patients with SIADH. Not only cytokine reactions after SCT but also neurological disorders caused by SCT can cause SIADH following SCT and neurological sequelae. SIADH may be considered as a potentially important symptom of neurological disorders and a predictor of neurological sequelae.

In conclusion, we revealed the differences in SIADH clinical features between CBSCT and BMT/PBSCT treatments and the more frequent occurrence of neurological sequelae following SCT in survivors with than without SIADH. The onset of SIADH following SCT was assumed to be associated with cytokine reactions after SCT and/or other neurological disorders caused by SCT. Further analysis of a much larger number of patients with SIADH following SCT is needed to explore the mechanisms of SIADH developing after SCT and to appropriately manage such patients.

References

1 Abe T, Takaue Y, Okamoto Y, Yamaue T, Nakagawa R, Makimoto A *et al.* Syndrome of inappropriate antidiuretic hormone secretion (SIADH) in children undergoing high-dose chemotherapy and autologous peripheral blood stem cell transplantation. *Pediatr Hematol Oncol* 1995; **12**: 363–369.
2 Festuccia F, Polci R, Pugliese F, Gargiulo A, Cinotti GA, Menè P. Syndrome of inappropriate ADH secretion: a late complication of hemopoietic stem cell allograft. *G Ital Nefrol* 2002; **19**: 353–360.
3 Kobayashi R, Iguchi A, Nakajima M, Sato T, Yoshida M, Kaneda M *et al.* Hyponatremia and syndrome of inappropriate antidiuretic hormone secretion complicating stem cell transplantation. *Bone Marrow Transplant* 2004; **34**: 975–979.
4 Bartter FC, Schwartz WB. The syndrome of inappropriate secretion of antidiuretic hormone. *Am J Med* 1967; **42**: 790–806.
5 Sorensen JB, Andersen MK, Hansen HH. Syndrome of inappropriate secretion of antidiuretic hormone (SIADH) in malignant disease. *J Intern Med* 1995; **238**: 97–110.
6 Sica S, Cicconi S, Sorà F, Chiusolo P, Piccirillo N, Laurenti L *et al.* Inappropriate antidiuretic hormone secretion after high-dose thiotepa. *Bone Marrow Transplant* 1999; **24**: 571–572.
7 Liu RY, Unmehopa UA, Zhou JN, Swaab DF. Glucocorticoids suppress vasopressin gene expression in human suprachiasmatic nucleus. *J Steroid Biochem Mol Biol* 2006; **98**: 248–253.
8 Chubachi A, Miura I, Hatano Y, Ohshima A, Nishinari T, Miura AB. Syndrome of appropriate secretion of antidiuretic hormone in patients with lymphoma associated hemophagocytic syndrome. *Ann Hematol* 1995; **70**: 53–55.
9 Ciaudo M, Chauvenet L, Audouin J, Rossert J, Favier R, Horellou MH *et al.* Peripheral T-cell lymphoma with hemophagocytic histiocytosis localized to the bone marrow associated with inappropriate secretion of antidiuretic hormone. *Leukemia Lymphoma* 1995; **19**: 511–514.
10 Eliakim R, Vertman E, Shinhar E. Syndrome of inappropriate secretion of antidiuretic hormone in Hodgkin's disease. *Am J Med Sci* 1986; **291**: 126–127.
11 Kelton JG, Logue G. Inappropriate antidiuretic hormone complicating histiocytic lymphoma. *Arch Intern Med* 1979; **139**: 307–308.
12 Mastorakos G, Weber JS, Magiakou MA, Gunn H, Chrousos GP. Hypothalamic-pituitary-adrenal axis activation and stimulation of systemic vasopressin secretion by recombinant interleukin-6 in humans: potential implications for the syndrome of inappropriate vasopressin secretion. *J Clin Endocrinol Metab* 1994; **79**: 934–939.
13 Gionis D, Ilias I, Moustaki M, Mantzos E, Papadatos I, Koutras DA *et al.* Hypothalamic-pituitary-adrenal axis and interleukin-6 activity in children with head trauma and syndrome of inappropriate secretion of antidiuretic hormone. *J Pediatr Endocrinol Metab* 2003; **16**: 49–54.
14 Ghorbel MT, Sharman G, Leroux M, Barrett T, Donovan DM, Becker KG *et al.* Microarray analysis reveals interleukin-6 as a novel secretory product of the hypothalamo-neurohypophyseal system. *J Biol Chem* 2003; **278**: 19280–19285.
15 Nagler A, Bishara A, Brautbar C, Barak V. Dysregulation of inflammatory cytokines in unrelated bone marrow transplantation. *Cytokines Cell Mol Ther* 1998; **4**: 161–167.
16 Kishi Y, Kami M, Miyakoshi S, Kanda Y, Murashige N, Teshima T *et al.* Early immune reaction after reduced-intensity cord-blood transplantation for adult patients. *Transplantation* 2005; **80**: 34–40.
17 Narimatsu H, Terakura S, Matsuo K, Oba T, Uchida T, Iida H *et al.* Short-term methotrexate could reduce early immune reactions and improve outcomes in umbilical cord blood transplantation for adults. *Bone Marrow Transplant* 2007; **39**: 31–39.
18 Shimura N, Kim H, Sugimoto H, Aoyagi Y, Baba H, Kim S. Syndrome of inappropriate secretion of antidiuretic hormone as a complication of human herpesvirus-6 infection. *Pediatr Int* 2004; **46**: 497–498.
19 Okafuji T, Uchiyama H, Okabe N, Akatsuka J, Maekawa K. Syndrome of inappropriate secretion of antidiuretic hormone associated with exanthem subitum. *Pediatr Infect Dis J* 1997; **16**: 532–533.
20 de Brabander C, Cornelissen J, Smitt PA, Vecht CJ, van den Bent MJ. Increased incidence of neurological complications in patients receiving an allogenic bone marrow transplantation

from alternative donors. *J Neurol Neurosurg Psychiatry* 2000; **68**: 36–40.
21 Bleggi-Torres LF, de Medeiros BC, Werner B, Neto JZ, Loddo G, Pasquini R *et al.* Neuropathological findings after bone marrow transplantation: an autopsy study of 180 cases. *Bone Marrow Transplant* 2000; **25**: 301–307.
22 Weber C, Schaper J, Tibussek D, Adams O, MacKenzie CR, Dilloo D *et al.* Diagnostic and therapeutic implications of neurological complications following paediatric haematopoietic stem cell transplantation. *Bone Marrow Transplant* 2008; **41**: 253–259.
23 Drakos P, Weinberger M, Delukina M, Or R, Nagler A, Weinberg M. Inappropriate antidiuretic hormone secretion (SIADH) preceding skin manifestations of disseminated varicella zoster virus infection. *Bone Marrow Transplant* 1993; **11**: 407–408.
24 Szabó F, Horvath N, Seimon S, Hughes T. Inappropriate antidiuretic hormone secretion, abdominal pain and disseminated varicella-zoster virus infection: an unusual triad in a patient 6 months post mini-allogeneic peripheral stem cell transplant for chronic myeloid leukemia. *Bone Marrow Transplant* 2000; **26**: 231–233.
25 Sato H, Kamoi K, Saeki T, Yamazaki H, Koike T, Miyamura S *et al.* Syndrome of inappropriate secretion of antidiuretic hormone and thrombocytopenia caused by cytomegalovirus infection in a young immunocompetent woman. *Intern Med* 2004; **43**: 1177–1182.
26 Nagamitsu S, Okabayashi S, Dai S, Morimitsu Y, Murakami T, Matsuishi T *et al.* Neuroimaging and neuropathologic findings in AIDS patient with cytomegalovirus infection. *Intern Med* 1994; **33**: 158–162.
27 Azuma T, Narumi H, Kojima K, Nawa Y, Hara M. Hyponatremia during administration of tacrolimus in an allogeneic bone marrow transplant recipient. *Int J Hematol* 2003; **78**: 268–269.

European Journal of Haematology ISSN 0902-4441

ORIGINAL ARTICLE

Possible application of flow cytometry for evaluation of the structure and functional status of WASP in peripheral blood mononuclear cells

Masaru Nakajima[1,3], Masafumi Yamada[2], Koji Yamaguchi[3], Yukio Sakiyama[3], Atsushi Oda[4], David L. Nelson[5], Yasutaka Yawaka[1], Tadashi Ariga[2]

[1]Division of Oral Functional Science, Department of Dentistry for Children and Disabled Person, Hokkaido University Graduate School of Dental Medicine, Sapporo, Japan; [2]Department of Pediatrics, Hokkaido University Graduate School of Medicine, Sapporo, Japan; [3]Research Group of Human Gene Therapy, Hokkaido University, Graduate School of Medicine, Sapporo, Japan; [4]Department of Preventive Medicine, Hokkaido University School of Medicine, Sapporo, Japan; [5]National Institutes of Health, National Cancer Institute, Metabolism Branch, Bethesda, MD, USA

Abstract

The Wiskott-Aldrich syndrome protein (WASP), which is defective in Wiskott-Aldrich syndrome (WAS) patients, is an intracellular protein expressed in non-erythroid hematopoietic cells. Previously, we have established methods to detect intracellular WASP expression in peripheral blood mononuclear cells (PBMNCs) using flow cytometric analysis (FCM-WASP) and have revealed that WAS patients showed absent or very low level intracellular WASP expression in lymphocytes and monocytes, while a significant amount of WASP was detected in those of normal individuals. We applied these methods for diagnostic screening of WAS patients and WAS carriers, as well as to the evaluation of mixed chimera in WAS patients who had previously undergone hematopoietic stem cell transplantation. During these procedures, we have noticed that lymphocytes from normal control individuals showed dual positive peaks, while their monocytes invariably showed a single sharp WASP-positive peak. To investigate the basis of the dual positive peaks ($WASP^{low\text{-}bright}$ and $WASP^{high\text{-}bright}$), we characterized the constituent linage lymphocytes of these two WASP-positive populations. As a result, we found each $WASP^{low/high}$ population comprised different linage PBMNCs. Furthermore, we propose that the difference between the two WASP-positive peaks did not result from any difference in WASP expression in the cells, but rather from a difference in the structural and functional status of the WASP protein in the cells. It has been shown that WASP may exist in two forms; an activated or inactivated form. Thus, the structural and functional WASP status or configuration could be evaluated by flow cytometric analysis.

Key words Wiskott-Aldrich syndrome protein; flow cytometry; Wiskott-Aldrich syndrome; peripheral blood mononuclear cells

Correspondence Tadashi Ariga, Department of Pediatrics, Hokkaido University Graduate School of Medicine, Japan. Tel: +81-11-706-7153; Fax: +81-11-706-7898; e-mail: tada-ari@med.hokudai.ac.jp

Accepted for publication 19 October 2008

doi:10.1111/j.1600-0609.2008.01180.x

The Wiskott-Aldrich syndrome protein (WASP) is the causative molecule underlying WAS (1). WASP comprises 502 amino acid residues, and is encoded by the *WASP gene*, which is organized into 12 exons encompassing 9 kb gDNA, and is located on the X-chromosome at Xp11.23-p11.22 (2). WASP belongs to the growing family of WASP/Scar/WAVE cytoplasmic scaffolding proteins, which are involved in cytoskeleton remodeling and actin nucleation/polymerization in response to activation stimuli (3, 4). Recent studies have revealed that WASP interacts with a number of intracellular molecules and plays key roles in signal transduction and the regulation of actin-polymerization (5–9). Furthermore, on the basis of crystal structure studies of the WASP molecule, it has been shown that WASP is involved in an auto-inhibition and activation mechanism via intra-molecular conformation changes (10).

Loss of function mutations in the *WASP* genes causes WAS, and X-linked thrombocytopenia (XLT) (11, 12), while gain of function mutations in the WASP gene have shown to cause X-linked neutropenia (XLN) (13). However, the full extent of the varied clinical symptoms observed in these patients (14–20) has not been fully elucidated in relation to WASP abnormalities.

Previously, we have established methods to detect intracellular WASP expression in peripheral blood mononuclear cells (PBMNCs) by flow cytometric analysis (FCM-WASP) (21). We have applied the methods to the screening of WAS patients, for the identification of carrier (22–24), or for the evaluation of WAS patients after receiving hematopoietic stem cell transplantation (25) and finally to detection of spontaneous reversion of WAS cases (26). During these pervious FCM-WASP experiments, we have identified normal control individual lymphocytes that showed dual positive peaks (WASP$^{low\text{-}bright}$ and WASP$^{high\text{-}bright}$). In this study, we tried to characterize the constituent cell lineage members of these two distinct populations of normal lymphocytes as detected by FCM-WASP, and investigate the mechanism underlying the two populations. Here we demonstrate that the two WASP populations consist of different lineage lymphocytes, and the difference between the two WASP$^{low/high}$ lymphocyte populations seems to result from differences in the functional status of the WASP molecule in the cell.

Materials and methods

Anti-WASP antibodies

Two different anti-WASP antibodies were used in this study. One is 3F3A5 (1.2 mg/mL), unconjugated mouse-IgG1 monoclonal anti-WASP antibody (11), which was raised against recombinant WASP corresponding to amino acids 202–302. We used 3F3A5 for FCM-WASP with fluorescein isothiocyanate (FITC)-conjugated goat anti-mouse IgG1 antibody (Southern Biotechnology Associates, Birmingham, AL, USA, 1.0 mg/mL). The second antibody was B-9 (Santa Cruz Biotechnology, Inc, 200 μg/mL), a phycoerythrin (PE)-conjugated mouse monoclonal IgG2a antibody, which was raised against recombinant WASP corresponding to amino acids 1–250.

FCM-WASP

FCM-WASP was performed as previously described (21). In brief, PBMNCs were purified using Ficoll-Hypaque, and both the cell surface and cytoplasm were stained. For staining cytoplasmic WASP, cells were treated with Cytofix/Cytoperm solution from the CytoStain kit (Pharmingen, San Diego, CA, USA) at 4°C for 20 min. After two washes with Perm/Wash solution (Pharmingen), they were incubated with 200× diluted mouse anti-WASP antibody (3F3A5) or 5× diluted mouse IgG1 antibody (BectonDickinson, San Jose, CA, USA) at 4°C for 30 min. After washing in phosphate-buffer saline (PBS)-2% fetal bovine serum (P-2), they were incubated with 100× diluted goat anti-mouse IgG1-FITC antibody (Southern Biotechnology Associates) as the secondary antibody again at 4°C for 30 min. In some experiments, a second, 10× diluted different anti-WASP antibody (B-9) was used. We used 10× diluted PE-conjugated mouse IgG2 as an isotypic control antibody. For surface/intracellular dual staining using the 3F3A5 antibody, we first stained the cell surface, followed by washing twice before performing intracellular staining. Antibodies used for surface staining were as follows; 5 μL of PE-conjugated anti-CD4, 10 μL of anti-CD8, and 10 μL of anti-CD56 (Southern Biotechnology Associates); PE-conjugated 10 μL of anti-CD20 (Beckman Coulter, Fullerton, CA, USA); and 10 μL of PE-Cy5-conjugated anti-CD45RA and 10 μL of anti-CD45RO (eBioscience, San Diego, CA, USA). The antibodies or the cell surface staining were mouse IgG2 to avoid cross reactivity with the 100× diluted goat anti-mouse IgG1-FITC antibody. We washed it with P-2 twice and stained intracellular WASP as described above. Stained PBMNCs were analyzed by FACSCalibur (BD, San Jose, CA, USA), using CellQuest software (Becton Dickinson).

Simultaneous staining with the two anti-WASP antibodies

After fixation and permeabilization procedure, normal control individual lymphocytes were simultaneously stained with 3F3A5 and B-9 at 4°C for 30 min, followed by staining with goat anti-mouse IgG1-FITC, and then, FCM-WASP was performed. The two WASP antibodies were used at the same protein concentration.

CD3+/CD45RA+ and CD3+/CD45RO+ purification

The two populations of CD3+/CD45RA+ and CD3+/CD45RO+ were purified as follows. Twenty microliters of CD3, CD45RA or CD45RO MicroBeads (Miltenyi Biotec, Bergisch Gladbach, Germany) diluted with 80 μL of magnetic cell sorting (MACS) buffer (pH 7.2, PBS 0.5% BSA, 2 mM EDTA) were incubated with each batch of 10^7 lymphocytes at 4°C for 15 min, and then, these cells were washed in MACS buffer. Afterwards, the two populations prepared as above were separated with Vario MACS (Miltenyi Biotec) and an MS

column (Miltenyi Biotec). Each cell population was checked for purity by flow cytometry.

Western blot analysis

The CD3+CD45RA+ ($WASP^{low\text{-}bright}$) lineages and CD3+CD45RO+ ($WASP^{high\text{-}bright}$) cells were respectively dissolved in RIPA buffer (Sigma, St Louis, MO, USA) containing protease inhibitors at 4°C for 20 min and were centrifuged at 14 500 *g* at 4°C for 20 min. We completely dissolved the cells in SD sample buffer (Sigma) and after boiling the samples, the cell extract of comprising 5×10^6 equivalency was electrophoresed with 10% polyacrylamide gel and blotted on a Hybond-PPVDF membrane (Amersham, Buckinghamshire, UK). We then stained the membrane with 1000× diluted 3F3A5 and 250× diluted anti-WIP antibody (kindly provided by Dr Ramesh N. Children's Hospital, Harvard University, MA, USA) as a loading control, followed by 1000× diluted peroxidase-conjugated goat anti-mouse IgG and 1000× diluted peroxidase-conjugated goat anti-rabbit IgG, and then used the ECL detection system (Amersham, Aylesbury, UK) for the detection of bands.

RT-PCR analysis

Total RNA from CD3+CD45RA+cells or CD3+CD45RO+ cells was extracted using an RNA isolation solvent (RNA zolTM Cinna/Biotecx, Houston, TX, USA). Two micrograms each of total RNA was used for cDNA synthesis with the first-strand cDNA synthesis kit (Pharmacia LKB Biotechnology, Uppsala, Sweden) and then, the same volume of each part of cDNA product was PCR-amplified with a set of primers (forward: GAAGACAAGGGCAGAAAGCA, reverse: GGGTTATCCTTCACGAAGCA). We performed electrophoresis of the PCR products and photographed the bands stained with ethidium bromide in the gel under ultraviolet light.

FCM-WASP for CD8+ lymphocytes after *in vitro* short-term activation

The change of WASP-positive pattern in CD8+ lymphocytes was studied after *in vitro* short-term activation. CD8+ cells were purified in the following way. PBMNCs from normal individuals were incubated at 4°C with each 20 μL of CD4, CD56 and CD20 MicroBeads (Miltenyi Biotec) for 15 min, and cells were obtained after performing Vario MACS using an LD column and their purity was checked and used for the experiment. After *in vitro* short-term activation with ionomycin (25 ng/mL) and PMA (1 μg/mL) at 37°C for 4 h, CD8+ lymphocytes were performed FCM-WASP and analyzed by CellQuest software (Franklin Lakes, NJ, USA).

Results

Normal peripheral blood mononuclear cells showed two WASP-positive populations by FCM-WASP

We have detected two WASP-positive populations; $WASP^{low\text{-}bright}$ and $WASP^{high\text{-}bright}$, in normal PBMNCs using 3F3A5. In monocytes, these two distinct populations have never been detected, but only low-bright positive have been previously described. The pattern of these dual positive peaks showed some variation among individuals (Fig. 1). We first studied the pattern of the two WASP-positive populations in the different lymphocyte lineages including; CD4+, CD8+, CD20+, CD56+. The results showed that CD20+ cells were $WASP^{low\text{-}bright}$, whereas CD56+ cells were $WASP^{high\text{-}bright}$. In cases of CD4+ and CD8+ cell lineages, both $WASP^{low/high}$ positive peaks were observed. We subsequently studied the pattern of WASP in CD4+/CD45RA+ or CD45RO+ and CD8+/CD45RA+ or CD45RO+ lymphocytes. This demonstrated that CD45RO+ cells that were either CD4+ or CD8+ were $WASP^{high\text{-}bright}$, and that CD45RA+ cells with either CD4+ or CD8+ showed $WASP^{low\text{-}bright}$ (Fig. 2).

Simultaneous staining with two anti-WASP antibodies revealed that the two WASP-positive peaks were detected with 3F3A5, but not with B-9 using

The two lymphocyte WASP-positive peaks observed using FCM-WASP were repeatedly detected using 3F3A5, but not with the B-9 antibody. To clarify these findings, we performed FCM-WASP on normal lymphocytes with simultaneous staining with 3F3A5 and B-9. The results clearly showed that the two WASP-positive peaks could be detected only with 3F3A5, but not with B-9 (Fig. 3A).

No differences in the amount of WASP protein, or WASP mRNA levels were detected between $WASP^{low\text{-}bright}$ and $WASP^{high\text{-}bright}$ cell populations

We isolated the CD3+/CD45RA+ lymphocyte population as $WASP^{low\text{-}bright}$ cells, and CD3+/CD45RO+ population as $WASP^{high\text{-}bright}$ cells. We compared the amount of WASP protein and message levels between these two cell populations. We used WIP as a loading protein control and glyceraldehyde-3-phosphate dehydrogenase as a standard cDNA control. No obvious differences were observed at the WASP protein (Fig. 4A) or message levels (Fig. 4B) between the two populations.

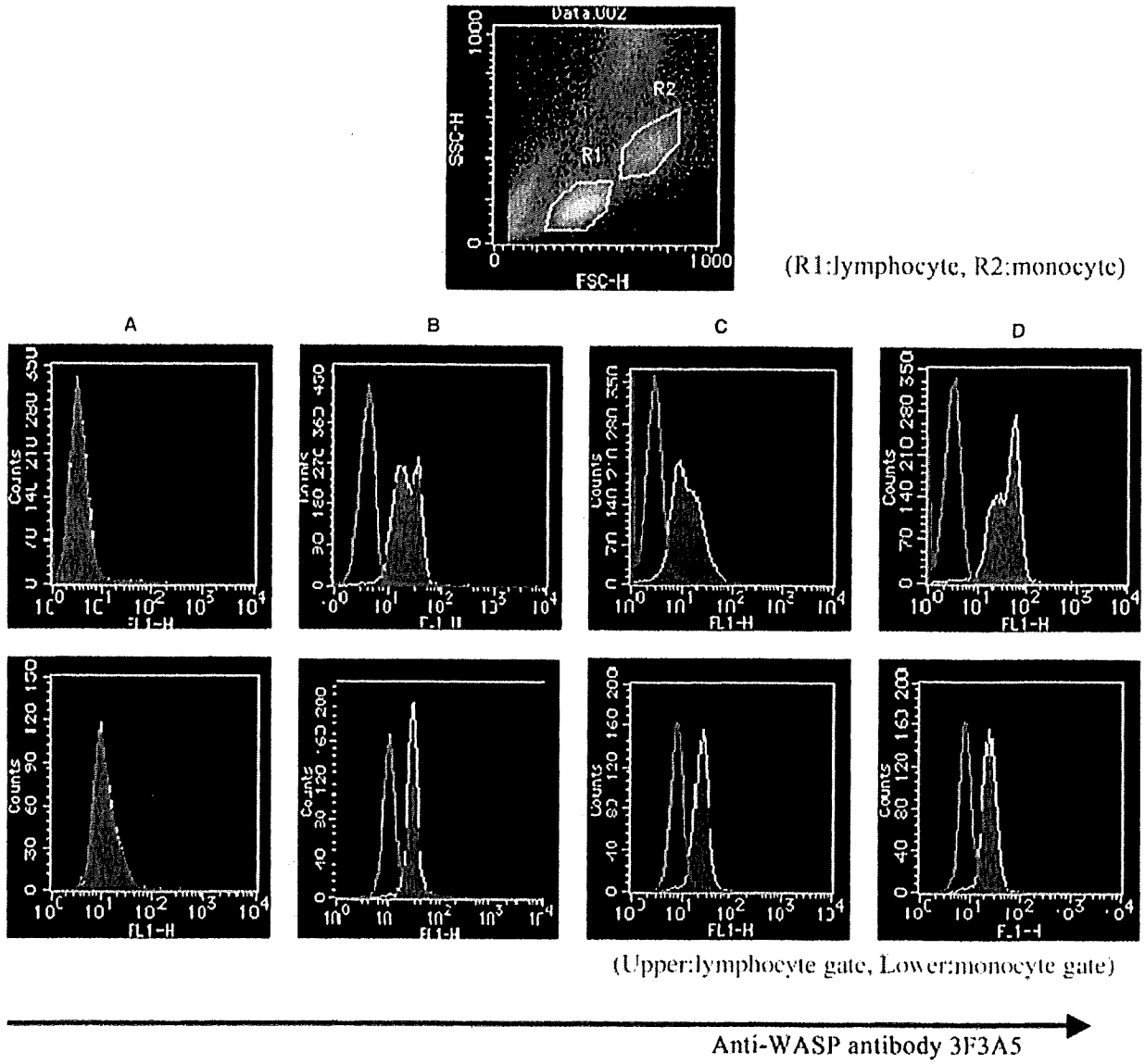

Figure 1 Two WASP-positive populations were detected in lymphocytes by FCM-WASP. Using the anti-WASP antibody 3F3A5, a pattern of two WASP-positive populations; $WASP^{high\text{-}bright}$ cells and $WASP^{low\text{-}bright}$, were observed in lymphocytes from normal individuals. In contrast, monocytes from the same individuals showed only a single WASP-positive population. (A) a patient with WAS, (B–D) normal control individuals. The top figure shows analysis of the lymphocyte gate (R1), and the monocyte gate (R2). The middle 4 figures show the results of lymphocytes, the lower 4 figures show the results of monocytes.

The WASP-positive pattern in CD8+ lymphocytes as seen by FCM-WASP changed during *in vitro* short-term activation

We next studied the effects of short-term lymphocyte activation on the WASP-positive cell pattern by FCM-WASP in the same lineage cells. We used CD8+ lymphocytes, because the CD8+ lineage has two populations most remarkably. To avoid synthesis of new WASP during activation, we settled on using a short-term (4 h) *in vitro* activation system and used 3F3A5 and B-9 antibodies together with FCM-WASP. We purified CD8+ lymphocytes by negative selection and these cells were used for FCM-WASP after PMA/ionomycin stimulation. After the short-term stimulation, the WASP-positive pattern showed significant up-regulation in FCM-WASP using 3F3A5, but not in FCM-WASP using B-9 (Fig. 5).

Discussion

In our previous studies, we noticed that lymphocytes from healthy individuals showed two WASP expression

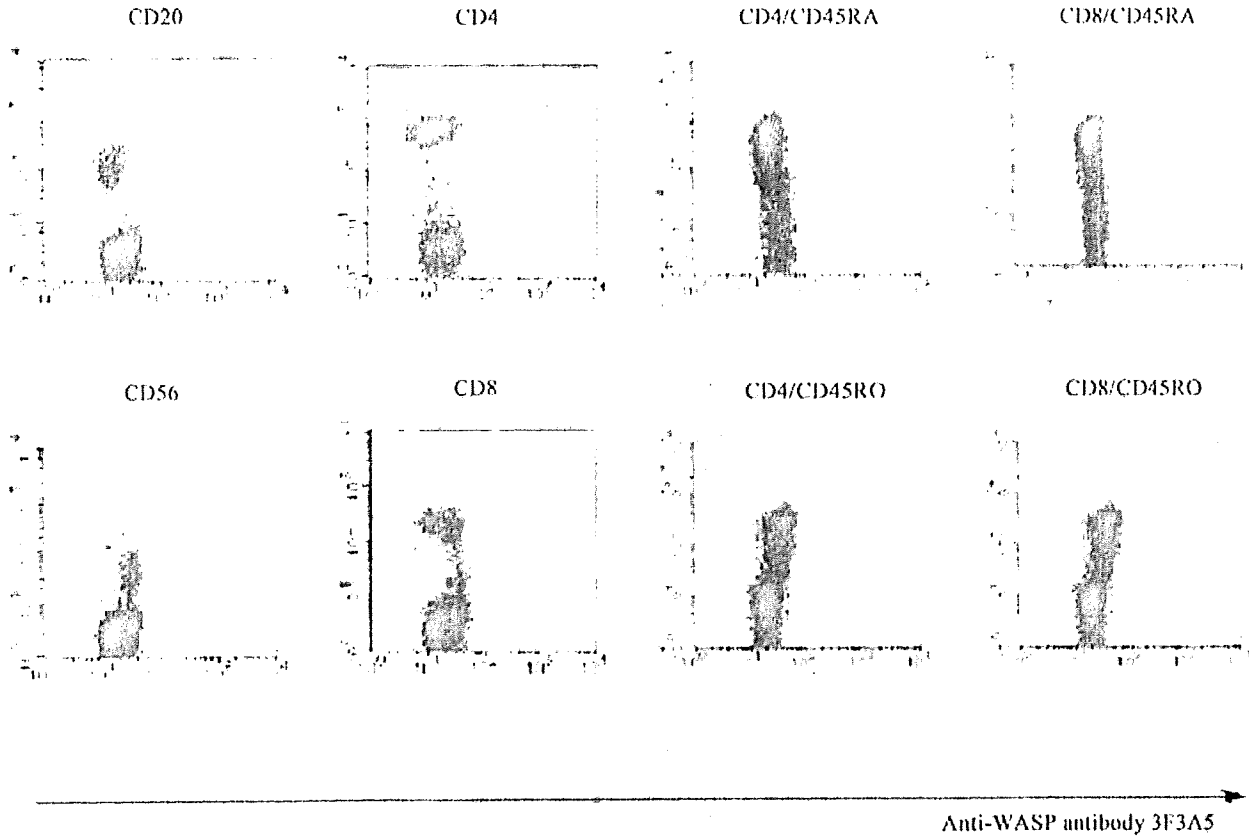

Figure 2 Characterization of the constituent cell lineages of the each WASP-positive population. By dual/triple staining of intracellular WASP and surface cell markers, we determined that CD20+, CD4+/CD45RA+ and CD8+/CD45RA+ cells belonged to the WASP$^{low\text{-}bright}$ population, whereas CD56+, CD4+/CD45RO+ and CD8+/CD45RO+ cells belonged to WASP$^{high\text{-}bright}$

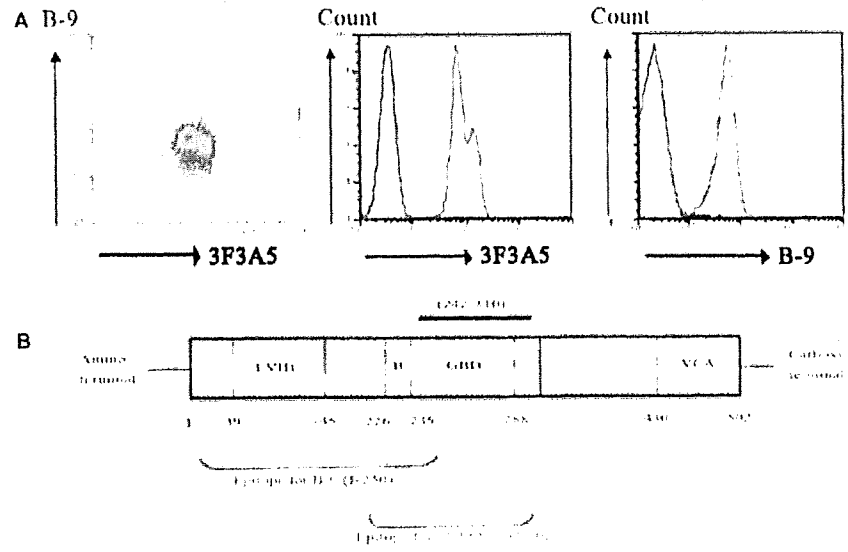

Figure 3 FCM-WASP after simultaneous staining with two different anti-WASP antibodies; 3F3A5 and B-9 (A). The top figure indicates the results of simultaneous analysis with 3F3A5 and B-9, showing two distinct subpopulations using the 3F3A5 antibody, but a single positive population by B-9. The lower two figures show each independent result. The scheme showing the WASP structure (B) Figures indicate amino acid number The underlined region (242–310) highlights a part of the GBD domain that is thought to be used for binding to the VCA domain in the inactive form of WASP. The scheme includes areas of possible epitopes for B-9 and 3F3A5 antibody binding represented. GBD domain (amino acids 235~288) is included within the 3F3A5 recognition site (amino acids 202–302).

profile populations; WASP$^{low\text{-}bright}$ and WASP$^{high\text{-}bright}$, using FCM-WASP. In this study, we confirmed two WASP-positive cell populations detected in the normal lymphocyte populations using FCM-WASP, and have proposed a possible mechanism causing the two populations.

We characterized the constituent cell lineage members of the each WASP-positive population. It was found that

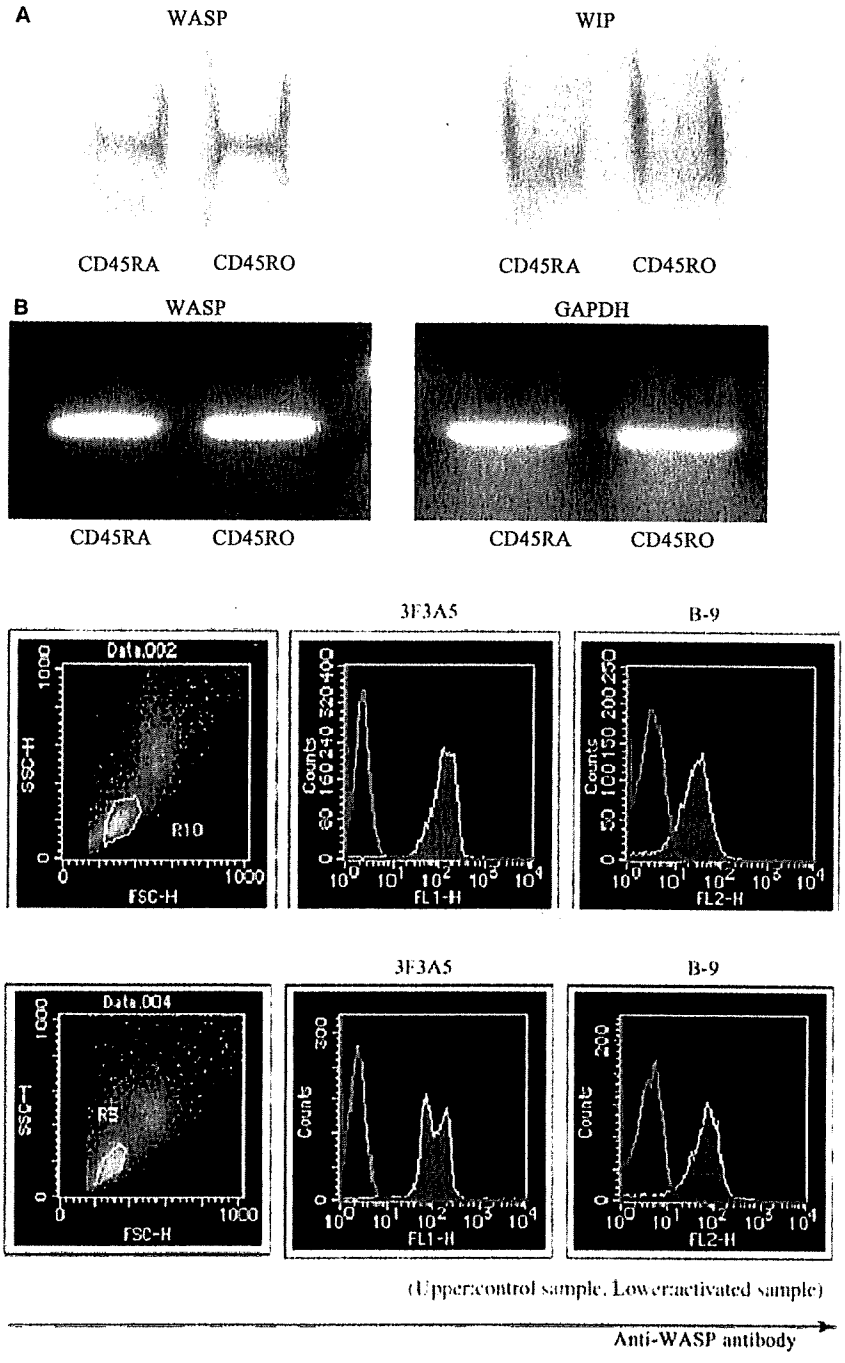

Figure 4 Protein and message levels of WASP in CD3+CD45RA+ cells and CD3+CD45RO+ cells. No significant difference in WASP protein or message levels was observed between $WASP^{low\text{-}bright}$ (CD3+/CD45RA+) and $WASP^{high\text{-}bright}$ (CD3+/CD45RO+) populations. We used WIP as a loading protein control and glyceraldehyde-3-phosphate dehydrogenase (GAPDH) as a standard cDNA control. (A) Western blot analysis. (B) Reverse transcriptase (RT)-PCR analysis

Figure 5 Effects of short-term activation on the WASP expression pattern in CD8+ cells analyzed using FCM-WASP. Purified CD8+ cells were incubated with or without activation for 4 h and the WASP-expression patterns are compared by FCM-WASP. Using the 3F3A5 antibody, the pattern was clearly changed upon activation. In contrast, this postactivation pattern showed no change using B-9.

monocytes, CD20+ cells, CD4+/CD45RA+ cells and CD8+/CD45RA+ cells belonged to the $WASP^{low\text{-}bright}$ population, whereas CD56+ cells, CD4+/CD45RO+ cells and CD8+/CD45RO+ cells belonged to the $WASP^{high\text{-}bright}$ group. It is interesting that these results seem to be linked to the hierarchy of WASP dependency for cell proliferation/survival; which we have proposed based on various aspects of studies on WAS patients and their families. These studies included WAS carrier analysis (21, 22), mixed chimera analysis in WAS patients after hematopoietic stem cell transplantation (25) and cell lineage analysis in WAS patients who showed somatic mosaicism due to spontaneous reversion to normal from inherited mutations (26). Based on these results, we speculated that WASP-dependency was lower in monocytes and B cells compared to T cells, and among T cells, naïve T cells were less WASP dependent than memory T cells. Although we cannot accurately place the requirements for NK cells in this hierarchy for WASP dependency, recent reports suggested that NK cell WASP

dependency seemed high (27, 28). Thus, those less WASP dependent cells belong to the WASP $^{low\text{-}bright}$ population, while highly WASP dependent cells belong to the WASP$^{high\text{-}bright}$ population. This consistency suggests that the difference between the two WASP-positive populations is linked to the difference in the response of these cells through WASP-mediated stimulations.

Next, we studied the basis of differences between the two WASP-positive populations. Differences in WASP staining dot brightness as demonstrated by flow cytometry are generally considered as differences in the quantity of molecules detected by antibodies. Unexpectedly, however, we found that the two WASP-positive lymphocyte populations detected by FCM-WASP were only identified using the 3F3A5 antibody, but not with the B-9 antibody, which was confirmed by simultaneous staining with 3F3A5 and B-9 (Fig. 3A). These results indicate that the difference between WASP$^{low\text{-}bright}$ and WASP$^{high\text{-}bright}$ cells results not from any disparity in WASP expression, but from disparity in antibody binding to WASP that is likely dependant on protein confirmation. Accordingly, we purified CD3+/CD45RA+ and CD3+/CD45RO+ cells, representing WASP$^{low\text{-}bright}$ and WASP$^{high\text{-}bright}$ populations respectively, and performed Western blot and RT-PCR analysis. The results showed there was no apparent difference in WASP or *WASP* mRNA levels between them (Fig. 4A,B), supporting the speculation that there is no disparity in WASP expression between lymphocytes showing WASP$^{low\text{-}bright}$ and WASP$^{high\text{-}bright}$ staining patterns.

Recently, WASP autoinhibition and activation mechanisms have been reported (10). The crystal structure model of the WASP, indicated that it could exist in either an activated or an inactivated form based on intramolecular structural changes. WASP has an N-terminal Ena/VASP homology domain 1 (EVH1) domain, a Cdc42/Rac GTPase binding domain (GBD), a proline-rich domain, a G-actin binding verprolin homology (V) domain, a cofilin homology (C) domain and a C-terminal acidic (A) segment.

WASP interacts with Cdc42-GTP via its GBD, with multiple SH3 domain-containing proteins that include Nck via its proline-rich region, with actin and the ARP2/3 complex via its VCA domain. WASP is usually present in cells in a closed, inactive conformation due to intramolecular regulatory interactions that involve the C-terminal acidic domain and the basic region that precedes the GBD. Binding of Cdc42-GTP is thought to cause WASP conformational change, which allows the VCA domain to interact with and activate the Arp2/3 complex (10) (Fig. 3B).

Based on these auto-inactivation and activation mechanisms of WASP, we speculate that the results from the two WASP-positive lymphocyte populations detected by FCM-WASP are related to this mechanism. As shown in Fig. 4, the two WASP-positive lymphocyte populations were detected with anti-WASP antibody 3F3A5, not with B-9. The WASP epitopes recognized by these two antibodies are different; 3F3A5 recognizes an epitope within amino acids 202~302 of WASP (this region includes the GBD), whereas the B-9 antibody recognizes an epitope lying within 1~250 amino acids of WASP (11). It is important to note that a part of the GBD (amino acids 235~288), that is hypothesized to be involved in binding to the VCA domain in the inactive form of WASP, might be included in the 3F3A5 antibody recognition site. Thus, we propose that the 3F3A5 antibody might be able to be used to distinguish a structural or activation state change in WASP, that is not possible using the B-9 antibody.

Finally, we studied the effects of short-term activation on the WASP-positive pattern by FCM-WASP in these CD8+ lineage cells. To avoid new WASP synthesis, we cultured cells for short term *in vitro* activation (4 h). Our data revealed that short-term activation forced a dramatic change to the WASP$^{high\text{-}bright}$ pattern in the same cell lineage (Fig. 5).

Here we report a new possible application of flow cytometry for analysis of intracellular WAS protein and its structural and functional status. However, from our data we cannot determine the relation or possible function of the two WASP-positive populations and their relationship to their WASP activation or inactivation status. Further different aspects of studies, such as FCM-WASP for patients with XLN, will be needed to answer these questions.

Acknowledgements

This study was supported by Grant-in-aid for Scientific Research from the Japanese Ministry of Health, Labor and Welfare (2542002917, 15COE011-02 and H19-Child-General-003).

References

1. Stewart DM, Tian L, Nelson DL. Mutations that cause the Wiskott-Aldrich syndrome impair the interaction of Wiskott-Aldrich syndrome protein (WASP) with WASP interacting protein. *J Immunol* 1999;**162**:5019–24.
2. Derry JMJ, Ochs HD, Francke U. Isolation of a novel gene mutated in Wiskott-Aldrich syndrome. *Cell* 1994;**78**:635–44.
3. Symons M, Derry JMJ, Karlak B, Jiang S, Lemahieu V, Mccormick F, Francke U, Abo A. Wiskott-Aldrich syndrome protein, a novel effector for the GTPase CDC42Hs, is implicated in actin polymerization. *Cell* 1996;**84**:723–34.

4. Molina IJ, Sancho J, Terhorst C, Rosen FS, Remoid-O'Donnell E. T cells of patients with the Wiskott-Aldrich syndrome have a restricted defect in proliferative responses. *J Immunol* 1993;**151**:4383–90.
5. Cory GOC, MacCarthy-Morrogh L, Banin S, Gout I, Brickell PM, Levinsky RI, Kinnon C, Lovering RC. Evidence that the Wiskott-Aldrich syndrome protein may be involved in lymphoid cell signaling pathways. *J Immunol* 1996;**157**:3791–5.
6. Rudolph MG, Bayer P, Abo A, Kuhlmann J, Vetter IR, Wittinghofer A. The CDC42/Racinteractive binding region motif of the Wiskott-Aldrich syndrome protein (WASP) is necessary but not sufficient for tight binding to CDC42 and structure formation. *J Biol Chem* 1998;**273**:18067–76.
7. Higgs HN, Pollard TD. Regulation of actin filament network formation through arp2/3 complex: activation by a diverse array of proteins. *Annu Rev Biochem* 2001;**70**:649–76.
8. Gallego MD, Santamaria M, Pena J, Molina IJ. Defective actin reorganization and polymerization of Wiskott-Aldrich syndrome T cells in response to CD3-mediated stimulation. *Blood* 1997;**90**:3089–97.
9. Candotti F, Facchetti F, Blanzuoli L, Stewart DM, Nelson DL, Blaese RM. Retrovirus-mediated WASP gene transfer corrects defective actin polymerization in cell lines from Wiskott-Aldrich syndrome patients carrying null mutations. *Gene Ther* 1999;**6**:1170–4.
10. Kim AS, Kakalis LT, Abdul-Manan N, Liu GA, Rosen MK. Autoinhibition and activation mechanism of the Wiskott-Aldrich syndrome protein. *Nature* 2000;**404**:151–8.
11. Stewart DM, Treiber-Held S, Kurman CC, Facchetti F, Notarangelo LD, Nelson DL. Studies of the expression of the Wiskott-Aldrich syndrome protein. *J Clin Invest* 1996;**97**:2627–34.
12. Derry JMJ, Kerns JA, Weinberg KI, Ochs HD, Volpini V, Estivill X, Walker AP, Franke U. WASP gene mutations in Wiskott-Aldrich syndrome and X-linked thrombocytopenia. *Hum Mol Genet* 1995;**4**:1127–35.
13. Devriendt K, Kim AS, Mathijs G, *et al.* Constitutively activating mutation in WASP causes X-linked severe congenital neutropenia. *Nat Genet* 2001;**27**:313–7.
14. Aldrich RA, Steinber AG, Campbell DC. Pedigree demonstrating a sex-linked recessive condition characterized by draining ears, eczematoid dermatitis and bloody diarrhea. *Pediatrics.* 1954;**13**:133–9.
15. Sullivan KE, Mullen CA, Blaese RM, Winkeistein JA. A multi-institutional survey of the Wiskott-Aldrich syndrome. *J Pediatr* 1994;**125**:876–85.
16. Ochs HD. The Wiskott-Aldrich syndrome. *Semin Hematol* 1998;**35**:332–45.
17. Oda A, Ochs HD. Wiskott-Aldrich syndrome protein and platelets. *Immunol Rev* 2000;**178**:111–7.
18. Lutskiy MI, Rosen FS, Remold-O'Donnell E. Genotype-proteotype linkage in the Wiskott-Aldrich syndrome. *J Immunol* 2005;**175**:1329–36.
19. Folwaczny C, Ruelfs C, Walther J, König A, Emmerich B. Ulcerative colitis in a patient with Wiskott-Aldrich syndrome. *Endoscopy* 2005;**34**:840–1.
20. Johnston SL, Unsworth DJ, Dwight JF, Kennedy CTC. Wiskott-Aldrich syndrome, vasculitis and critical aortic dilatation. *Acta Paediatr* 2002;**90**:1346–8.
21. Yamada M, Ohtsu M, Kobayashi I, *et al.* Flow cytometric analysis of Wiskott-Aldrich syndrome (WAS) protein in lymphocytes from WAS patients and their familial carriers. *Blood* 1999;**93**:756–62.
22. Yamada M, Ariga T, Kawamura N, *et al.* Determination of carrier status for the Wiskott-Aldrich syndrome by flow cytometric analysis of Wiskott-Aldrich protein expression in peripheral blood mononuclear cells. *J Immunol* 2000;**165**:1119–22.
23. Ariga T, Yamada M, Wada T, Saitoh S, Sakiyama Y. Detection of lymphocytes and granulocytes expressing the mutant WASP message in carriers of Wiskott-Aldrich syndrome. *Br J Haematol* 1999;**104**:893–900.
24. Ariga T, Yamada M, Sakiyama Y. Mutation analysis of five Japanese families with Wiskott-Aldrich syndrome and determination of the family members'carrier status using three different methods. *Pediatr Res* 1997;**41**:535–40.
25. Yamaguchi K, Ariga T, Yamada M, *et al.* Mixed chimera status of 12 patient with Wiskott-Aldrich syndrome (WAS) after hematopoietic stem cell transplantation; evaluation by flow cytometric analysis of intracellular WAS protein expression. *Blood* 2002;**100**:1208–14.
26. Ariga T, Kondoh T, Yamaguchi K, Yamada M, Sasaki S, Nelson DL, Ikeda H, Kobayashi K, Moriuchi H, Sakiyama Y. Spontaneous in vivo reversion of an inherited mutation in the Wiskott-Aldrich syndrome. *J Immunol* 2001;**166**:5245–9.
27. Lutskiy MI, Beardsley DS, Rosen FS, Remold-O'Donnell E. Mosaicism of NK cells in a patient with Wiskott-Aldrich syndrome. *Blood* 2005;**106**:2815–7.
28. Orange JS, Ramesh N, Remold-O'Donnell E, Sasahara Y, Koopman L, Byrne M, Bonilla FA, Rosen FS, Geha RS, Strominger JL. Wiskott-Aldrich syndrome protein is required for NK cell cytotoxicity and colocalizes with actin to NK cell-activating immunologic synapses. *Proc Natl Acad Sci USA* 2002;**99**:11351–6.

Identification of Severe Combined Immunodeficiency by T-Cell Receptor Excision Circles Quantification Using Neonatal Guthrie Cards

Yoichi Morinishi, MD, PhD, Kohsuke Imai, MD, PhD, Noriko Nakagawa, MD, Hiroki Sato, MHSc, Katsuyuki Horiuchi, MD, PhD, Yoshitoshi Ohtsuka, MD, PhD, Yumi Kaneda, MD, Takashi Taga, MD, PhD, Hiroaki Hisakawa, MD, PhD, Ryosuke Miyaji, MD, Mikiya Endo, MD, Tsutomu Oh–ishi, MD, PhD, Yoshiro Kamachi, MD, PhD, Koshi Akahane, MD, Chie Kobayashi, MD, PhD, Masahiro Tsuchida, MD, PhD, Tomohiro Morio, MD, PhD, Yoji Sasahara, MD, PhD, Satoru Kumaki, MD, PhD, Keiko Ishigaki, MD, PhD, Makoto Yoshida, MD, PhD, Tomonari Urabe, MD, Norimoto Kobayashi, MD, PhD, Yuri Okimoto, MD, PhD, Janine Reichenbach, MD, PhD, Yoshiko Hashii, MD, PhD, Yoichiro Tsuji, MD, PhD, Kazuhiro Kogawa, MD, PhD, Seiji Yamaguchi, MD, PhD, Hirokazu Kanegane, MD, PhD, Toshio Miyawaki, MD, PhD, Masafumi Yamada, MD, PhD, Tadashi Ariga, MD, PhD, and Shigeaki Nonoyama, MD, PhD

Objective To assess the feasibility of T-cell receptor excision circles (TRECs) quantification for neonatal mass screening of severe combined immunodeficiency (SCID).

Study design Real-time PCR based quantification of TRECs for 471 healthy control patients and 18 patients with SCID with various genetic abnormalities (*IL2RG*, *JAK3*, *ADA*, *LIG4*, *RAG1*) were performed, including patients with maternal T-cell engraftment (n = 4) and leaky T cells (n = 3).

Results TRECs were detectable in all normal neonatal Guthrie cards (n = 326) at the levels of 10^4 to 10^5 copies/μg DNA. In contrast, TRECs were extremely low in all neonatal Guthrie cards (n = 15) and peripheral blood (n = 14) from patients with SCID, including those with maternal T-cell engraftment or leaky T cells with hypomorphic RAG1 mutations or LIG4 deficiency. There were no false-positive or negative results in this study.

Conclusion TRECs quantification can be used as a neonatal mass screening for patients with SCID. *(J Pediatr 2009;155:829-33).*

See related article, p 834

Severe combined immunodeficiency (SCID) is a genetic disorder characterized by the absence of T-cells and adaptive immunity.[1,2] Affected infants usually have severe infections due to opportunistic pathogens in the first months of life. Hematopoietic stem cell transplantation can reconstitute immune function, although severe infections before hematopoietic stem cell transplantation can be fatal to the patients within the first year of life.[3,4] Thus, early diagnosis before the occurrence of severe infection is essential.[5-7]

Four different mechanisms have been identified as a cause of SCID, including purine metabolism defects, defective signaling of the common γ-chain–dependent cytokine receptors, defective V(D)J recombination, and defective pre-TCR/TCR signaling.[1,2] Although human SCID is caused by mutations of at least 10 different genes, all patients have a characteristic decreased number of newly

BCG	Bacillus Calmette-Guérin
BMT	Bone marrow transplantation
CMV	Cytomegalovirus
FISH	Fluorescent in situ hybridization
HSCT	Hematopoietic stem cell transplantation
PB	Peripheral blood
PCR	Polymerase chain reaction
sjTRECs	Signal joint TRECs
SCID	Severe combined immunodeficiency
TCR	T-cell receptor
TRECs	T-cell receptor excision circles
UCB	Umbilical cord blood

From the Department of Pediatrics (Y.M., K.I., N.N., K.H., Y.T., K.K., S.N.), National Defense Medical College, Saitama, Japan; the Department of Medical Informatics (K.I., H.S.), National Defense Medical College Hospital, Saitama, Japan; the Department of Pediatrics (Y.O., Y.K.), Hyogo College of Medicine, Hyogo, Japan; Department of Pediatrics (T.T.), Shiga University of Medical Science, Shiga, Japan; the Department of Pediatrics (H.H.), Kochi University, Kochi, Japan; the Department of Pediatrics (R.M.), University of Occupational and Environmental Health, Fukuoka, Japan; the Department of Pediatrics (M.E.), Iwate Medical University, Iwate, Japan; the Division of Infectious Diseases, Immunology, and Allergy (T.O.), Saitama Children's Medical Center, Saitama, Japan; the Department of Pediatrics (Y.K.), Nagoya University Graduate School of Medicine, Aichi, Japan; the Department of Pediatrics (K.A.), Yamanashi Prefectural Central Hospital, Yamanashi, Japan; the Department of Pediatrics (C.K., M.T.), Ibaraki Children's Hospital, Ibaraki, Japan; the Department of Pediatrics (T.M.), Tokyo Medical and Dental University, Tokyo, Japan; the Department of Pediatrics (Y.S., S.K.), Tohoku University, Miyagi, Japan; the Department of Pediatrics (K.I.), Tokyo Women's Medical University, Tokyo, Japan; the Department of Pediatrics (M.Y.), Asahikawa Medical College, Hokkaido, Japan; the Department of Pediatrics (T.U.), Kumamoto University, Kumamoto, Japan; the Department of Interdisciplinary Medicine (N.K.), Nagano Children's Hospital, Nagano, Japan; the Department of Hematology/Oncology (Y.O.), Chiba Children's Hospital, Chiba, Japan; the Department of Immunology/Hematology/BMT (J.R.), University Children's Hospital Zurich, Zurich, Switzerland; the Department of Pediatrics (Y.H.), Osaka University, Osaka, Japan; the Department of Pediatrics (S.Y.), Shimane University, Shimane, Japan; the Department of Pediatrics (H.K., T.M.), University of Toyama, Toyama, Japan; and the Department of Pediatrics (M.Y., T.A.), Hokkaido University, Hokkaido, Japan

Supported by grants from the Ministry of Defense, Ministry of Health, Labour and Welfare Kawano Masanori Foundation for Promotion of Pediatrics, Jeffrey Modell Foundation, and The Mother and Child Health Foundation. The authors declare no conflicts of interest.

 10.1016/j.jpeds.2009.05.026

Table. Genotype, lymphocyte subset, and TRECs of patients with SCID

Patient	Sex	Genotype	Age at onset of symptoms	Age at SCID diagnosis	Lymphocytes (/μL)	CD3+ (%)	CD3+ (/μL)	CD19+ (%)	CD45RO+ / CD4 + CD3 + (%)	Maternal lymphocyte engraftment	Guthrie cards TRECs (/μg DNA)	PB Pre-HSCT TRECs (/μg DNA)	PB Pre-HSCT Age
1	M	*IL2RG*	3 mo	3 mo	720	0.0	0	-	86.0	-	<10	-	-
2	M	*IL2RG*	-	0 mo	780	0.0	0	-	94.0	-	<10	<10	0 y, 0 mo
3	M	*IL2RG*	-	0 mo	920	0.0	0	-	91.0	-	<10	<10	0 y, 0 mo
4	M	*IL2RG*	4 mo	5 mo	2550	0.2	5	NA	99.4	-	<10	<10	0 y, 5 mo
5	M	*IL2RG*	10 mo	10 mo	1035	0.0	0	-	94.7	-	<10	<10	0 y, 10 mo
6	M	*IL2RG*	4 mo	5 mo	3560	0.0	0	-	95.8	-	<10	<10	0 y, 5 mo
7	M	*IL2RG*	-	0 mo	966	0.7	7	95.3	77.5	-	<10	<10	0 y, 0 mo
8	M	*JAK3*	4 mo	4 mo	3810	0.0	0	-	87.0	-	<10	-	-
9	F	*JAK3*	2 mo	5 mo	2495	0.0	0	-	89.8	-	<10	<10	0 y, 6 mo
10	M	*ADA*	1 mo	4 mo	90	40.0	36	99.5	4.4	-	<10	<10	0 y, 2 mo
11	M	*ADA*	1 mo	2 m	100	6.8	7	89.9	0.9	-	6.2×10^2	<10	0 y, 1 mo
12	M	*IL2RG*	8 mo	8 mo	3250	40.8	1326	89.8	65.5	T + NK+	-	<10	1 y
13	M	*IL2RG*	-	0 mo	950	4.2	40	NA	68.6	T+	<10	-	-
14	M	*IL2RG*	9 mo	10 mo	860	7.0	60	99.6	85.9	T + NK+	<10	<10	0 y, 10 mo
15	M	*IL2RG*	3 mo	3 mo	300	36.5	110	NA	53.5	T+	<10	-	-
16	F	*LIG4*	-	0 mo	550	38.7	213	97.6	0.3	-	-	<10	2 y
17	M	*LIG4*	1 y, 6 mo	4 y	300	44.3	133	25.2	0.1	-	<10	<10	4 y
18	F	*RAG1*	8 mo	1 y 9 mo	550	53.1	292	91.6	12.0	-	-	8.0×10^1	2 y

NA, Not available.

developed T cells.[1,2,8,9] T-cell receptor excision circles (TRECs) are small circular DNA fragments formed through rearrangement of the T-cell receptor (TCR) α locus and do not multiply during cell division.[9-13] Therefore, TRECs quantification is reportedly useful for determining recent thymic emigrants. Two reports of a method for neonatal screening of SCID using TRECs quantification by real-time PCR have been published.[6,7] Both studies quantified TRECs of patients with SCID using peripheral blood and found significantly lower levels of TRECs than those of control neonates. In addition, Guthrie cards from 2 patients with SCID retrospectively had undetectable TRECs.[6] Most control neonates had high amounts of TRECs. However, TRECs were undetectable in some samples. To increase specificity, 1 study[7] proposed a 2-tiered strategy using a combination of quantified TRECs and IL-7.

We have evaluated blood from Guthrie cards and peripheral blood from control patients and patients with SCID for detecting TRECs.

Methods

Peripheral blood samples were obtained from 112 healthy volunteers (median age, 14 years; range, 0.1 to 51 years). Thirty-three umbilical cord blood samples (median gestational age, 38.9 weeks) were collected at the National Defense Medical College Hospital. Dried blood spots of umbilical cord blood were obtained by applying 50 μL of residual blood to the 11-mm circles on filter-paper cards (PKU-S, Toyoroshi, Tokyo, Japan). Twenty-six neonatal Guthrie cards with dried blood spots were donated from surplus routine samples for newborn mass screening from neonates born at National Defense Medical College Hospital during this study period (January 2005 to December 2007). In addition, 300 neonatal Guthrie cards, stored at −20°C for less than 5 years in a neonatal mass screening center at Shimane University, were analyzed.

Eighteen patients with SCID were analyzed for TRECs (**Table**). All patients were genetically diagnosed using genomic DNA sequencing. Mutations of either *IL2RG* (n = 11), *JAK3* (n = 2), *RAG1* (n = 1), *ADA* (n = 2), or *LIG4* (n = 2) were identified in the patients (**Table**).

Peripheral blood samples of 14 patients before hematopoietic stem cell transplantation were used. In addition, neonatal Guthrie cards of 15 patients that had been stored in newborn mass screening centers were obtained.

Maternal T and NK lymphocyte engraftment was diagnosed by fluorescent in situ hybridization (FISH) using X and Y chromosome–specific probes after purification of each compartment by specific monoclonal antibodies and immunomagnetic beads.

The study protocol was approved by the National Defense Medical College Institutional Review Board, and informed consent was obtained from the parents of patients with SCID and healthy control patients, as well as adult control patients, in accordance with the Declaration of Helsinki.

Quantification of TRECs by Real-Time PCR

We used 100 μL of whole blood (EDTA anticoagulated peripheral blood and heparinized cord blood) or 2 punches of 6 mm in diameter from Guthrie card to extract genomic DNA.

Concentrations of DNA from peripheral blood, fresh dried blood punches from normal neonates (n = 26), and stored dried blood spots from normal neonates (n = 300) were

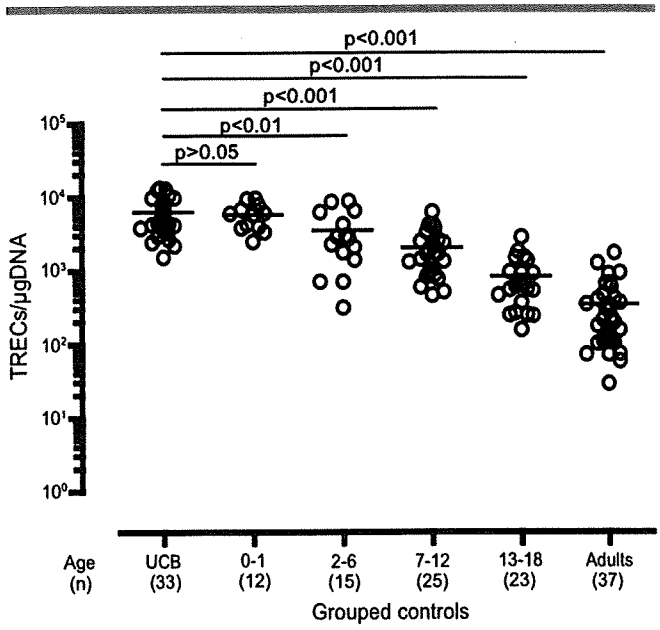

Figure 1. Umbilical cord blood (UCB) (n = 33) and peripheral blood (n = 112, 0 to 51 years) samples were analyzed. TRECs in different age groups are shown. TRECs were significantly higher in umbilical cord blood ($6.2 \pm 3.2 \times 10^3$ copies/μg DNA) and infants ($5.8 \pm 2.3 \times 10^3$ copies/μg DNA) as compared with other age groups of children ($3.5 \pm 2.8 \times 10^3$ copies/μg DNA in 2 to 6 years old, $2.0 \pm 1.4 \times 10^3$ copies/μg DNA in 7 to 12 years old, $8.2 \pm 6.3 \times 10^2$ copies/μg DNA in 13 to 18 years old) and adults ($3.4 \pm 3.6 \times 10^2$ copies/μg DNA).

40.6 ± 2.3 ng/μL (mean $\pm$ SEM) (range, 13 to 167 ng/μL), 7.8 ± 2.8 ng/μL (2.9 to 13.0 ng/μL), and 5.3 ± 0.2 ng/μL (0.6 to 20.2 ng/μL), respectively.

Quantitative real-time PCR for δRec-ψJα sjTRECs was performed using the same primers and δRec probes as reported by Hazenberg et al.[14]

As an internal control, RNaseP gene was amplified in each sample tested using TaqMan RNaseP Primer-Probe (VIC dye) Mix (Applied Biosystems, Foster City, California).

Statistical Analysis

An exponential regression model was used to quantify the relationship between age and TRECs levels (per μg DNA and per RNaseP). Goodness-of-fit of the model was evaluated by R^2. The Dunnett multiple comparison test was conducted to test the differences of each age group (0 to 1, 2 to 6, 7 to 12, 13 to 18 years and adults) versus umbilical cord blood comparisons serving as a control group (**Figure 1**). RNaseP and TRECs levels of patients with SCID and control patients were compared by an unpaired Student t test (if the variance was equal) or Welch t test (if the variance was different).

All statistical analyses were performed using GraphPad Prism Version 4.00 (GraphPad Software, San Diego, California). $P < .05$ denotes a statistically significant difference.

Results

TRECs were detectable in all DNA samples from whole blood of normal control patients, including umbilical cord blood (n = 33), healthy infants (0 to 1 year old, n = 12), children (2 to 18 years old, n = 63), and adults (n = 37). TRECs in whole blood were found to decline with increasing age ($r = 0.851$). TRECs of umbilical cord blood were significantly higher than those of children and adults but were not significantly different from those of infants (**Figure 1**). We found a strong correlation between TRECs copies/μg DNA and TRECs/RNaseP ratio ($r = 0.979$).

TRECs of peripheral blood samples from all 14 patients with SCID before hematopoietic stem cell transplantation were below detectable levels (<10 copies/μg DNA) with the exception of 1 (P18, see below), in contrast to high levels of control infants ($5.8 \pm 0.7 \times 10^3$/μg DNA, n = 12) ($P < .0001$) (**Figure 2**, A).

Next, we analyzed TRECs of dried blood spots from normal control neonates using simulated Guthrie cards from cord blood (n = 31), neonatal Guthrie cards obtained during this study period (January 2005 to December 2007) (n = 26), and those stored in a neonatal mass screening center for less than 5 years (n = 300). TRECs were detectable in all dried blood spots: in cord blood ($1.3 \pm 0.1 \times 10^4$ copies/μg DNA, mean $\pm$ SEM), in neonatal Guthrie cards ($2.3 \pm 0.2 \times 10^4$ copies/μg DNA), and in stored neonatal Guthrie cards ($3.6 \pm 0.2 \times 10^5$ copies/μg DNA).

To determine whether this method can identify patients with SCID, we quantified TRECs using 15 stored neonatal Guthrie cards from patients with SCID (patients 1 through 11, 13 through 15, and patient 17). RNaseP levels were high in all neonatal Guthrie cards from patients with SCID ($1.8 \pm 0.3 \times 10^6$ copies/μg DNA, n = 15), which were similar to control levels ($2.3 \pm 0.1 \times 10^6$ copies/μg DNA, n = 26) ($P = .184$), indicating an appropriate amount of genomic DNA was extracted from the neonatal Guthrie cards (**Figure 2**, B). In contrast, TRECs were below detection levels in all patients ($P < .0001$) except 1 (patient 11). This patient with SCID had compound heterozygous mutations of *ADA* (Gln119Stop/Arg34Ser). He had detectable but significantly lower levels of TRECs (6.2×10^2 copies/μg DNA) than those of control neonates ($2.3 \pm 0.2 \times 10^4$ copies/μg DNA, n = 26) (**Figure 2**, B). At 1 month of age, the TRECs from the peripheral blood of patient 11 were below detectable levels (**Table** and **Figure 2**, A).

These results indicate that neonatal mass screening of SCID by quantitative real-time PCR for TRECs using neonatal Guthrie cards is feasible.

We analyzed TRECs in 4 patients with SCID with maternal T-cell engraftment (patients 12 through 15, $CD3^+$ cells: 40 to 1326/μL). We found that all patients had undetectable levels of TRECs in neonatal Guthrie cards (patients 13 through 15) and peripheral blood (patients 12 and 14). Patient 12 had a normal lymphocyte count (3250/μL) on admission as well as a significant number of T, B, and NK cells (**Table**). His peripheral blood TRECs level was below the detection

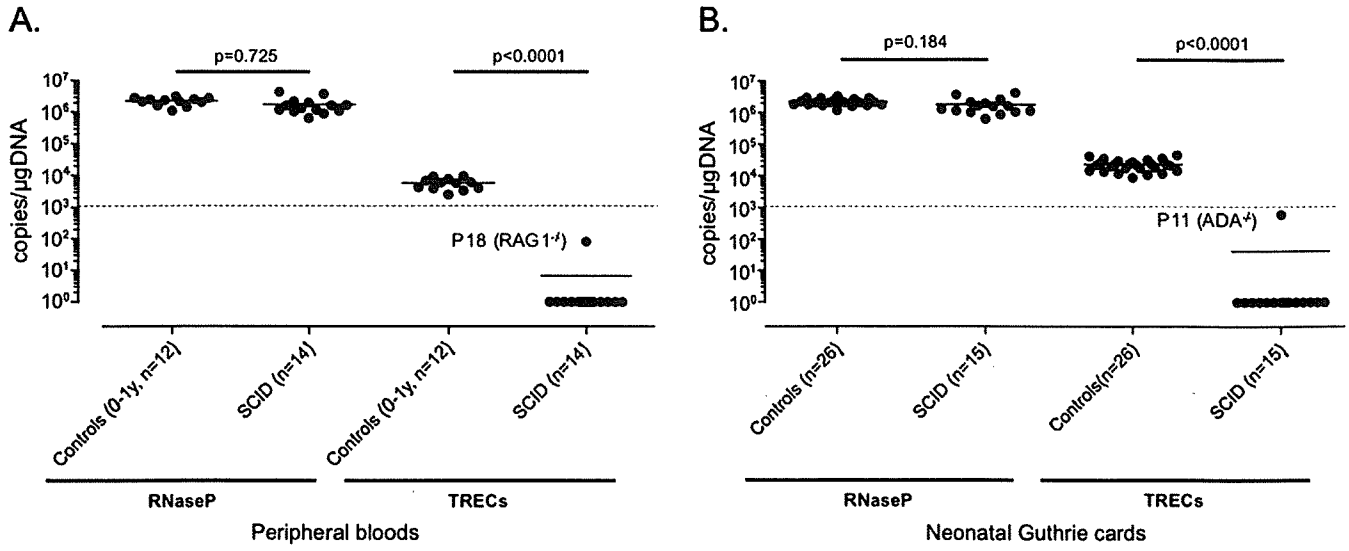

Figure 2. A, RNaseP levels in peripheral blood from patients with SCID ($2.1 \pm 0.2 \times 10^6$ copies/μg DNA, n = 14) were comparable with those from control infants ($2.2 \pm 0.2 \times 10^6$ copies/μg DNA, n = 12) ($P = .725$). Peripheral blood TRECs from all typical patients with SCID were undetectable (<10 copies/μg DNA) as compared with the high copy number of peripheral blood TRECs from control neonates ($5.8 \pm 0.7 \times 10^3$ copies/μg DNA, n = 12) ($P < .0001$). Patient 18, with hypomorphic RAG1 mutations, had detectable but extremely low TRECs in peripheral blood (8.0×10^1 copies/μg DNA). **B,** RNaseP levels in neonatal Guthrie cards from patients with SCID ($1.8 \pm 0.3 \times 10^6$ copies/μg DNA, n = 15) were comparable with those from control neonates ($2.3 \pm 0.1 \times 10^6$ copies/μg DNA, n = 26) ($P = .184$). TRECs of Guthrie cards from 14 of 15 patients with SCID during the early neonatal period were undetectable (<10 copies/μg DNA). An ADA-deficient patient ($ADA^{-/-}$, patient 11) had detectable but significantly low TRECs levels (6.2×10^2 copies/μg DNA) compared with control neonates ($2.3 \pm 0.2 \times 10^4$ copies/μg DNA, n = 26).

levels despite the presence of peripheral T cells. FISH analysis revealed that all circulating $CD3^+$ cells (1326/μL) were derived from his mother. Similarly, TRECs of other patients (patients 13 through 15) were also undetectable despite the maternal T cells (**Table**).

These results confirm the findings of Patel et al[9] indicating that TRECs quantification is both effective and reliable for the screening of SCID even in the presence of maternal T cells.

Patient 18 with hypomorphic *RAG1* mutations was lymphopenic (550/μL) at 21 months of age, but T (53.1%), B (12.0%), and NK cells (31.2%) were present in peripheral blood. Both T cells with TCR$\alpha\beta$ chain and TCR$\gamma\delta$ chain were derived from the patient, as determined by FISH analysis of the sex chromosome.

The peripheral blood TRECs from this patient (8.0×10^1 copies/μg DNA) (**Figure 2**, A) was significantly lower than age-matched control patients ($5.2 \pm 3.2 \times 10^3$ copies/μg DNA, n = 5). We purified T cells with TCR$\alpha\beta$ chain by FACS sorting. T cells with TCR$\alpha\beta$ from patient 18 had very low TRECs/cells (4.0×10^1 copies/10^5 cells) than those of age-matched control patients (5.1×10^3 copies/10^5 cells).

We also analyzed TRECs in 2 LIG4-deficient patients (patients 16 and 17) who had leaky T cells (**Table**). Peripheral blood TRECs were undetectable in both patients (**Figure 2**, A), and TRECs in the neonatal Guthrie card were also undetectable in patient 17 (**Figure 2**, B).

These results indicate that TRECs are extremely low in patients with SCID, even if leaky T cells are present.

Discussion

We demonstrated that TRECs were undetectable, or were significantly lower (10^1 to 10^2 copies/μg DNA) than healthy neonates and infants (10^4 to 10^5 copies/μg DNA), in both neonatal Guthrie cards and peripheral blood samples obtained from SCID. All types of SCID tested, including IL2RG, JAK3, ADA, RAG1, LIG4 deficiencies, were identified by measuring TRECs. This finding was consistent with the previous reports that showed the usefulness of TRECs for the identification of SCID[6,7,9] and further indicates that TRECs can identify SCID with maternal T cells and SCID with leaky T cells. In 2 LIG4-deficient patients with leaky T cells (CD3 + 38.7% and 44.3%) and in 1 patient with hypomorphic mutations in *RAG1* gene, who had immunodeficiency and autoimmunity with residual memory T cells,[15,16] TRECs were undetectable. These results indicate that TRECs is a good marker to identify the defect of V(D)J recombination, in which LIG4 and RAG1 play essential roles. We observed progressive loss of TRECs in a patient with SCID and ADA deficiency (patient 11). This observation is compatible with the report that the loss of naive T lymphocytes occurs after birth in patients with ADA deficiency.[17,18]

No false-negative was observed in this study (TRECs were below normal range in all cases of SCID), although sample size was too small to determine the exact false-negative rate.

Consistently, there were no false-positive (TRECs were all positive) in the control samples in this study. The previous studies showed 2.9% and 7.7% of false-positive rates.[6,7] The primers and probe used in this study [14] were different from previously studies.[6,7] However, both probes were found to result in equivalent quantities (data not shown). Thus, the reason of the different false-positive rate between this and the previous studies is currently undetermined. Mass screening using larger population will disclose the exact false-positive and false-negative rate.

The cost to test 1 sample in our study is $5 per sample, which was reported to be cost-effective.[19] We are now trying to further reduce the cost.

Early diagnosis of SCID can prevent severe and recurrent infection, which is often fatal and makes stem cell transplantation difficult. Identification of SCID by newborn screening by TRECs will improve the prognosis and quality of life of patients with SCID. ■

We thank the patients and their families who participated in this study. We also thank Mrs Makiko Tanaka for her skillful technical assistance and members of Department of Obstetrics and Gynecology, National Defense Medical College for collecting umbilical cord blood samples.

Submitted for publication Oct 10, 2008; last revision received April 22, 2009; accepted May 19, 2009.

Reprint requests: Dr Kohsuke Imai, National Defense Medical College, 3-2 Namiki, Tokorozawa, Saitama, Japan, 359-8513. E-mail: kimai@ndmc.ac.jp.

References

1. Fischer A, Le Deist F, Hacein-Bey-Abina S, Andre-Schmutz I, BasileGde S, de Villartay JP, et al. Severe combined immunodeficiency: a model disease for molecular immunology and therapy. Immunol Rev 2005;203:98-109.
2. Buckley RH. Molecular defects in human severe combined immunodeficiency and approaches to immune reconstitution. Annu Rev Immunol 2004;22:625-55.
3. Buckley RH, Schiff SE, Schiff RI, Markert L, Williams LW, Roberts JL, et al. Hematopoietic stem-cell transplantation for the treatment of severe combined immunodeficiency. N Engl J Med 1999;340:508-16.
4. Antoine C, Muller S, Cant A, Cavazzana-Calvo M, Veys P, Vossen J, et al. Long-term survival and transplantation of haemopoietic stem cells for immunodeficiencies: report of the European experience 1968-99. Lancet 2003;361:553-60.
5. Myers LA, Patel DD, Puck JM, Buckley RH. Hematopoietic stem cell transplantation for severe combined immunodeficiency in the neonatal period leads to superior thymic output and improved survival. Blood 2002;99:872-8.
6. Chan K, Puck JM. Development of population-based newborn screening for severe combined immunodeficiency. J Allergy Clin Immunol 2005; 115:391-8.
7. McGhee SA, Stiehm ER, Cowan M, Krogstad P, McCabe ER. Two-tiered universal newborn screening strategy for severe combined immunodeficiency. Mol Genet Metab 2005;86:427-30.
8. Buckley RH, Schiff RI, Schiff SE, Markert ML, Williams LW, Harville TO, et al. Human severe combined immunodeficiency: genetic, phenotypic, and functional diversity in one hundred eight infants. J Pediatr 1997;130:378-87.
9. Patel DD, Gooding ME, Parrott RE, Curtis KM, Haynes BF, Buckley RH. Thymic function after hematopoietic stem-cell transplantation for the treatment of severe combined immunodeficiency. N Engl J Med 2000; 342:1325-32.
10. de Villartay JP, Hockett RD, Coran D, Korsmeyer SJ, Cohen DI. Deletion of the human T-cell receptor delta-gene by a site-specific recombination. Nature 1988;335:170-4.
11. Douek DC, McFarland RD, Keiser PH, Gage EA, Massey JM, Haynes BF, et al. Changes in thymic function with age and during the treatment of HIV infection. Nature 1998;396:690-5.
12. McFarland RD, Douek DC, Koup RA, Picker LJ. Identification of a human recent thymic emigrant phenotype. Proc Natl Acad Sci U S A 2000;97:4215-20.
13. Hazenberg MD, Verschuren MC, Hamann D, Miedema F, van Dongen JJ. T cell receptor excision circles as markers for recent thymic emigrants: basic aspects, technical approach, and guidelines for interpretation. J Mol Med 2001;79:631-40.
14. Hazenberg MD, Otto SA, CohenStuart JW, Verschuren MC, Borleffs JC, Boucher CA, et al. Increased cell division but not thymic dysfunction rapidly affects the T-cell receptor excision circle content of the naive T cell population in HIV-1 infection. Nat Med 2000;6: 1036-42.
15. de Villartay JP, Lim A, Al-Mousa H, Dupont S, Dechanet-Merville J, Coumau-Gatbois E, et al. A novel immunodeficiency associated with hypomorphic RAG1 mutations and CMV infection. J Clin Invest 2005;115: 3291-9.
16. Ehl S, Schwarz K, Enders A, Duffner U, Pannicke U, Kuhr J, et al. A variant of SCID with specific immune responses and predominance of gamma delta T cells. J Clin Invest 2005;115:3140-8.
17. Giblett ER, Anderson JE, Cohen F, Pollara B, Meuwissen HJ. Adenosine-deaminase deficiency in two patients with severely impaired cellular immunity. Lancet 1972;2:1067-9.
18. Hershfield MS. Genotype is an important determinant of phenotype in adenosine deaminase deficiency. Curr Opin Immunol 2003;15:571-7.
19. McGhee SA, Stiehm ER, McCabe ER. Potential costs and benefits of newborn screening for severe combined immunodeficiency. J Pediatr 2005; 147:603-8.

Two Candidate Tumor Suppressor Genes, *MEOX2* and *SOSTDC1*, Identified in a 7p21 Homozygous Deletion Region in a Wilms Tumor

Junjiro Ohshima,[1,2] Masayuki Haruta,[1] Yasuhito Arai,[3] Fumio Kasai,[1] Yuiko Fujiwara,[1] Tadashi Ariga,[2] Hajime Okita,[4] Masahiro Fukuzawa,[4] Jun-Ichi Hata,[4] Hiroshi Horie,[4] and Yasuhiko Kaneko[1,4]*

[1]Research Institute for Clinical Oncology, Saitama Cancer Center, Ina, Saitama, Japan
[2]Department of Pediatrics, Hokkaido University School of Medicine, Sapporo, Japan
[3]Cancer Genomics Project, National Cancer Center Research Institute, Chuo-Ku, Tokyo, Japan
[4]Japan Wilms Tumor Study Group (JWiTS), Itabashi-Ku, Tokyo, Japan

A SNP-based array analysis of 100 Wilms tumors (WT) from 97 patients identified 7p alterations (hemizygous and homozygous deletions and uniparental disomy) in nine tumors. The homozygous deletion (HD) region of 7p21 found in one tumor partially overlapped with another HD region reported previously, and was narrowed down to a 2.1-Mb region. Based on an expression analysis of 10 genes located in the HD region in 3 WT lines and previous studies on tumorigenic roles of *MEOX2* and *SOSTDC1*, we further analyzed these two genes. Sequencing showed no mutation in *MEOX2*, but two missense mutations (L50F and Q129L) in *SOSTDC1* in four tumors; L50F in two tumors was of germline origin. Expression levels (0, 1+ and 2+) of *MEOX2* were lower in four tumors with 7p alterations than in 18 tumors with no 7p alterations ($P = 0.017$), and those of *SOSTDC1* tended to be lower in five tumors with 7p alterations or *SOSTDC1* mutation than in 17 tumors with no 7p alterations or *SOSTDC1* mutation ($P = 0.056$). There were no significant differences in clinical characteristics between nine patients with 7p alterations and 88 patients with no 7p alterations; however, there was a difference in the status of *IGF2* (uniparental disomy, loss of imprinting, or retention of imprinting) between the two patient groups ($P = 0.028$). Losses of *MEOX2* and *SOSTDC1* may accelerate angiogenesis and augment signals in the Wnt pathway, respectively. Both genes may be prime candidates for 7p tumor suppressor genes, which may have a role in the progression of Wilms tumorigenesis.

INTRODUCTION

Wilms tumor (WT) (OMIM 194070) is one of the most common pediatric malignancies, accounting for 8% of childhood cancers and occurring in 1 in 10,000 children. The development of WT has been associated with abnormalities of genes or chromosomal regions, which are involved in the development of the embryonic kidney. The abnormalities include *WT1* located at 11p13, *IGF2*, and *H19* at 11p15.5, *WTX* at Xq11, 16q (*WT3*), 17q12-q21 (*WT4*), and 7p21-p11.2 (*WT5*) (Perlman et al., 2004; Rivera and Haber 2005; Rivera et al., 2007); however, deletion or mutation of *WT1* and *WTX* has been found in only 15–33% and 7–24%, respectively (Haruta et al., 2008; Perotti et al., 2008; Ruteshouser et al., 2008; Fukuzawa et al., 2009), and loss of imprinting (LOI) of *IGF2* in 40–70% of tumors (Ravenel et al., 2001; Yuan et al., 2005). Although WT is thought to arise according to the original paradigms of Knudson's two-hit model (Knudson and Strong, 1972), it has become apparent that several known and unknown genetic events also contribute to Wilms tumorigenesis.

Previous cytogenetic, loss of heterozygosity (LOH), and comparative genomic hybridization (CGH) studies indicated alterations of the short arm of Chromosome 7 in a substantial number (10–25%) of WTs (Wang-Wuu et al., 1990; Kaneko et al., 1991; Grundy et al., 1998; Powlesland et al., 2000; Sossey-Alaoui et al., 2003; Yuan et al., 2005), and suggested the presence of tumor suppressor genes in the deleted region. The *POU6F2* gene at 7p14.1 (Perotti

Supported by: The Ministry of Education, Science, Sports and Culture, Japan, Grant number: 1879074; The Ministry of Health, Labor, and Welfare, Japan for Third-term Comprehensive Control Research for Cancer; Kawano Masanori Memorial Foundation for Promotion of Pediatrics..

*Correspondence to: Yasuhiko Kaneko, Research Institute for Clinical Oncology, Saitama Cancer Center, 818 Komuro, Ina, Saitama 362-0806, Japan. E-mail: kaneko@cancer-c.pref.saitama.jp

Received 8 May 2009; Accepted 2 August 2009

DOI 10.1002/gcc.20705

Published online 16 September 2009 in Wiley InterScience (www.interscience.wiley.com).

et al., 2004) and *PTH-B1* at 7p14.3 (Vernon et al., 2003) have been proposed as 7p (*WT5*) genes, however; the roles of the two genes in Wilms tumorigenesis have not been fully elucidated. In addition, previous studies proposed another 7p region (7p22-p15) where candidate 7p genes reside (Grundy et al., 1998; Powlesland et al., 2000).

The single nucleotide polymorphism (SNP) array is a newly developed tool that can detect hemizygous and homozygous chromosomal deletions and uniparental disomy (UPD), and is superior to previous microsatellite markers for detecting LOH that could not distinguish deletions from UPD (Nannya et al., 2005; Yuan et al., 2005; Haruta et al., 2008). The detection of a small homozygous deletion (HD) has been crucial for the identification of tumor suppressor genes (Gessler et al., 1990), and use of the SNP array is the most suitable way to detect such a deletion (Northcott et al., 2009). An analysis of the present series of 100 WTs showed 7p loss or UPD in nine tumors, one of which had a HD region of 4.3 Mb at 7p21.3-p21.1. The region overlaps with a homozygously deleted region reported in a WT by Sossey-Alaoui et al., (2003), and was narrowed down to an area of 2.1 Mb. Of the eight genes within the HD region, we identified two, *MEOX2* (mesenchyme homeobox 2) and *SOSTDC1* (sclerostin domain-containing-1), as candidate tumor suppressor genes involved in Wilms tumorigenesis.

MATERIALS AND METHODS

Patients and Samples

One hundred WTs were obtained from 97 Japanese infants or children; three pairs of tumors were obtained from three patients with bilateral WTs. Eight patients with malformations were syndromic; two with Drash syndrome, five with WAGR syndrome and one with urinary tract malformation, and all three patients with bilateral tumors were syndromic. The remaining 89 patients had no malformations and a unilateral sporadic tumor. Two (Nos. 1 and 100) of the 89 patients were identical twins and their tumors shared the same frameshift mutation in Exon 1 of *WT1*; one (No. 1) was reported as No. 36 in the paper by Haruta et al., (2008). The age at diagnosis ranged from 2 months to 15 years with a median of 2 years and 9 months. Tumors were staged at the time of initial biopsy or surgery, which was carried out between September 1986 and September 2004, according to the National Wilms' Tumor Study Group (NWTS) staging system (d'Angio et al., 1989).

In all cases, the diagnosis of WT was made with routine hematoxylin- and eosin-stained slides by pathologists at each institution or the JWiTS pathology panel according to the classification proposed by the Japanese Society of Pathology and/or the NWTS pathology panel (Beckwith and Palmer, 1978; Japanese Society of Pathology, 2008). Pathologists in each institution verified that the sample for molecular genetic analysis contained 70% or more tumor cells. Three cell lines derived from Wilms tumors (HFWT, Ishiwata et al., 1991; WiT49, Alami et al., 2003; and CCG99-11, a gift from Dr. Benjamin Tycko) were included for mutation, expression, and SNP array analyses of the candidate genes. Normal samples were obtained from either peripheral blood or normal renal tissue adjacent to the tumor from 21 of 97 patients. The status of *WT1*, *IGF2*, and *CTNNB1* was analyzed as previously reported (Haruta et al., 2008). The ethics committee of Saitama Cancer Center approved the study design.

Copy Number and LOH Analysis Using SNP Arrays and Quantitative Real-Time PCR

High-resolution SNP arrays, Affymetrix Mapping 50K-*Xba* and 250K-*Nsp* arrays (Affymetrix, Santa Clara, CA), were used to analyze the chromosomal copy number and LOH status in 100 tumors as described previously (Nannya et al., 2005; Haruta et al., 2008). The analysis detected a HD at 7p21 in one tumor (No. 1), and the copy number of six genes within or close to the HD region was validated in this tumor by real-time quantitative PCR using a LightCycler (Roche Diagnostics, Indianapolis, IN). Primers and probes designed to specifically amplify the six genes or a reference gene, *MOCS2*, at 5q11 are listed in Table 1.

Mutation Analysis of the *MEOX2* and *SOSTDC1* Genes

To detect point mutations and deletions of the two candidate genes, *MEOX2* and *SOSTDC1*, genomic DNA from each tumor sample or cell line was amplified using four or two sets of primers (Table 2). PCR products were directly sequenced with the BigDye Terminator v3.1

Available online at www.sciencedirect.com
ScienceDirect
Blood Cells, Molecules, and Diseases 40 (2008) 410–413
BLOOD CELLS, MOLECULES, & DISEASES
www.elsevier.com/locate/ybcmd

The first confirmed case with C3 deficiency caused by compound heterozygous mutations in the *C3* gene; a new aspect of pathogenesis for C3 deficiency

Miyuki Kida [a], Hirotaka Fujioka [b], Yoshiyuki Kosaka [c], Kouhei Hayashi [c], Yukio Sakiyama [d], Tadashi Ariga [a,*]

[a] *Department of Pediatrics, Hokkaido University Graduate School of Medicine, N-15, W-7, Kita-ku, Sapporo, Hokkaido, Japan*
[b] *Department of Plastic Surgery, Bibai Rousai Hospital, Hokkaido, Japan*
[c] *Department of Hematology and Oncology, Hyogo Prefectural Kobe Children's Hospital, Hyogo, Japan*
[d] *Department of Human Gene Therapy, Hokkaido University Graduate School of Medicine, Hokkaido, Japan*

Submitted 29 October 2007
Available online 16 January 2008
(Communicated by R.I. Handin, M.D., 2 November 2007)

Abstract

The complement system is an ancient cascade system that has a major role in innate and adaptive immunity. Component C3 is central to the three complement pathways. Hereditary compliment 3 (C3) deficiency characterized by severe recurrent infections and immune complex disorders is extremely rare disease. Since 1972, inherited C3 deficiency has been described in many families representing a variety of national origins; however, only 8 families of these cases have been identified their genetic defects. Interestingly, all except one (incomplete analysis) were shown to harbor homozygous *C3* gene mutations. Previously we proposed a hypothesis, based on the unique process of C3 synthesis; C3 deficiency is not inherited as a simple autosomal recessive trait. Here, we report the first confirmed case with C3 deficiency caused by compound heterozygous mutations. They were a novel one base insertion (3176insT) in exon 24 which is predicted to result in a frameshift and a premature downstream stop codon (K1105X) in exon 26, and a nonsense mutation of C3303G (Y1081X) in exon 26 which was previously reported as homozygous mutations. This confirmed case suggests that our proposed hypothesis has prospects of a new aspect of pathogenesis for C3 deficiency.

Keywords: Component C3; C3 deficiency; Compound heterozygous mutations

Introduction

Complement protein C3 (OMIM+120700) is the major protein in the complement system in plasma. Cloning of the *C3* gene (19p13.3–13.2) revealed that the precursor molecule consists of 1663 amino acids encompassed by 41 exons and is located on chromosome 19. Inherited deficiency of C3 is an extremely rare disease; thus far, only 10 patients from eight families have had their molecular defects identified which led to their C3 deficiency [1–8]. It is notable that almost all mutations, which vary among each family group, were homozygous [1–4,6–8]. At present, only two cases (from one family) were suspected as being caused by compound heterozygous mutations after an incomplete analysis [5]. C3 is synthesized through a unique process; the mature C3 molecule results from a C3 precursor, which is cleaved into the α and β chains, and then the two chains are subsequently liked by disulfide bonds [9]. Previously, we reported the 10th case with C3 deficiency that was due to a novel homozygous mutation, and proposed a pathogenetic hypothesis, based on the unique process of C3 synthesis, that C3 deficiency is not inherited as a simple autosomal recessive trait [3]. Some compound heterozygous mutations, such as some combinations of missense mutations

* Corresponding author. Fax: +81 11 706 7898.
E-mail address: tada-ari@med.hokudai.ac.jp (T. Ariga).

1079-9796/$ - see front matter © 2007 Elsevier Inc. All rights reserved.
doi:10.1016/j.bcmd.2007.11.002